Journal of Power Sources 196 (2011) 8874–8880

Contents lists available at ScienceDirect

Journal of Power Sources

journal homepage: www.elsevier.com/locate/jpowsour

Comparison of solar cell performance of conducting polymer dyes with different functional groups

Jang-Hee Yoon [b], Dong-Min Kim [a], Sang-Su Yoon [a], Mi-Sook Won [b,*], Yoon-Bo Shim [a,*]

[a] Department of Chemistry, Pusan National University, Busan 609-735, South Korea
[b] Busan Center, Korea Basic Science Institute, Busan 609-735, South Korea

ARTICLE INFO

Article history:
Received 25 February 2011
Received in revised form 27 April 2011
Accepted 27 May 2011
Available online 21 June 2011

Keywords:
Conducting polymer dye
Nanocrystalline titanium dioxide
Solar cell

ABSTRACT

Conductive polymer precursors, including carboxylic acid, cyano groups, amino groups, 5,2′:5′,2″-terthiophene–3′-carboxylic acid (TTCA), 3′-cyano-5,2′:5′,2″-terthiophene (CTT), and 3′,4′-diamino-2,2′:5′,2″-terthiophene (DATT) are synthesized. Electrochemically polymerized films of the precursors on a nanocrystalline TiO_2 layer are examined as photo sensitizers, and the cell performance is compared. The photovoltaic cells are assembled with a polymer-coated TiO_2 layer treated with $TiCl_4$ as an anode and a Pt layer as a cathode in a propionitrile solution containing an iodide ion-based redox electrolyte. The charge-transfer processes of polymer-dyed cells are studied using impedance spectroscopy. The polymer dyes on the TiO_2 surfaces are characterized by scanning electron microscope (SEM), atomic force microscope (AFM), transmission electron microscope (TEM), and X-ray photoelectron spectroscopy (XPS). XPS results show that the conducting polymer dye, bearing a carboxylic acid group, is more strongly bound to the TiO_2 layer in comparison with other groups. Various experimental parameters affecting the cell efficiency are optimized, including the scan rate, number of potential cycles, and terthiophene monomer concentration. Of these polymers, the best cell efficiency is attained for poly-TTCA containing a carboxylic acid group. The optimized cell with the poly-TTCA dye shows a short-circuit current of 6.78 mA cm^{-2}, an open-circuit voltage of 0.54 V, and a fill factor of 63.6. An energy conversion efficiency of 2.32% is obtained with a cell area of 0.24 cm^2 under an air mass 1.5 solar simulated light irradiation of 100 mW cm^{-2}.

1. Introduction

Silicon-based solar cells are commercially available due to their high solar-to-electric energy conversion efficiency. They are associated with several disadvantages, however, including heavy weight, high cost and lack of flexibility. Several approaches, including the development of organic photovoltaic cells [1] and dye-sensitized solar cells (DSSCs) [2], have been introduced to overcome these disadvantages. DSSCs have a maximum energy conversion efficiency of ~10% [3]. The most successful sensitizer for DSSCs is a ruthenium complex that is anchored to a nanocrystalline TiO_2 surface via carboxylic acid groups. The ruthenium complex dyes are also associated with disadvantages, however, including high cost, low long-term availability, and lack of environmental safety. Several organic dyes, such as perylene, cyanine, xanthene, merocyanine, coumarin, hemicyanine, indoline, and triphenylamine have been studied as metal-free organic sensitizers for DSSCs [4]. The conjugated polymers, poly(*p*-phenylene vinylene)s and poly(thiophene)s have also been reported as sensitizers in DSSCs [5].

Poly(terthiophenes) are especially attractive as sensitizers in DSSCs because the heteroaromatic and extended π-conjugated backbone structure provide high environmental stability, electrical conductivity, and other attractive physical properties. The photoelectrochemical properties of poly(thiophene) [6–9], poly(bithiophene) [10], and poly(terthiophene) [11,12] have been explored as sensitizers in nanocrystalline TiO_2 photovoltaic cells. Of these, photovoltaic cells based on poly(terthiophene) have improved conjugation lengths and perform better than cells that are based on poly(thiophene) (or poly(bithiophene)) [13]. To date, the best energy conversion efficiency of these polymer dye cells is approximately 1.5% using poly(3-thiophene acetic acid) [6]. The energy conversion efficiency of thiophene-based conjugate polymer sensitizers is lower than those of ruthenium complex dyes. However, there have been a number of recent studies focused on improving the performance of thiophene derivatives. Most thiophene-based conjugated polymers do not have carboxylic acid groups; this result in disadvantages in dye adsorption and charge transfer process between the sensitizer and TiO_2. To promote efficiency using the conducting polymer (poly(terthiophene)),

* Corresponding authors. Tel.: +82 51 510 2244/2986; fax: +82 51 510 2430/517 2497.
E-mail addresses: mswon@kbsi.re.kr (M.-S. Won), ybshim@pusan.ac.kr (Y.-B. Shim).

0378-7753/$ – see front matter © 2011 Elsevier B.V. All rights reserved.
doi:10.1016/j.jpowsour.2011.05.077

functionalization of the polymer backbone seems promising, and new properties are being discovered. The role of the carboxylic acid groups on the polymer backbone has attracted attention for the developing an efficient ligand for adsorption onto TiO_2 [14–16]. A terthiophene monomeric unit that is functionalized at the 3′-position can be polymerized; the polymerization reaction is driven by the relief of steric hindrance. This may result from the bulky functional group in close proximity to the polymerization reaction site. Hence, the study of polymer backbones bearing three different types of functional groups, −COOH, $-NH_2$, and −CN, is a valuable method for comparing the effects of functional groups on the efficiencies of the polymer sensitizers.

In the present study, the effects of various functional groups bound to the poly(terthiophene) backbone on the efficiency and the resulting photovoltaic performance of solar cells were investigated with a nanocrystalline TiO_2 anode. The polymer dye/$TiCl_4$/TiO_2 surfaces were characterized by scanning electron microscope (SEM), atomic force microscope (AFM), transmittance electron microscope (TEM), and X-ray photon spectroscopy (XPS). The electropolymerization conditions (scan rate, potential cycling times, and monomer concentration) were optimized to obtain high-energy conversion efficiencies. The highest occupied molecular orbital (HOMO), the lowest unoccupied molecular orbital (LUMO), and the band gap energy of poly-TTCA were determined using cyclic voltammetry and UV–visible spectroscopy. Electrochemical impedance spectroscopy (EIS) was also used to investigate the charge-transfer processes of various polymer dye solar cells. Finally, the optimum conditions were investigated to prepare the best-performing photovoltaic cell based on the polymer sensitizer.

2. Experimental procedures

2.1. Synthesis of monomers

The terthiophene monomer, 3′-cyano-5,2′:5′,2″-terthiophene (CTT), 5,2′:5′,2″-terthiophene-3′-carboxylic acid (TTCA), and 3′,4′-diamino-2,2′:5′,2″-terthiophene (DATT) were synthesized according to previously reported procedures, as shown in Fig. 1 [17,18]. TTCA was synthesized from 3′-bromo-5,2′:5′,2″-terthiophene (BTT) by a two-step process. BTT was refluxed with cuprous cyanide (CuCN) in dimethylformamide to produce CTT in 89% yield. Mp: 83.0–84.0 °C. IR (KBr) 2217 cm^{-1}; ^1H NMR (300 MHz, $CDCl_3$) δ: 7.06–7.62 (m, 7H), ^{13}C NMR (75 MHz, $CDCl_3$) δ: 106.0, 115.8, 125.6, 125.7, 126.5, 127.7, 128.0, 128.6, 128.8, 133.4, 135.0, 136.7, 145.3; MS mz^{-1} (rel intensity) 273 (M^+, 100%). The resulting CTT was hydrolyzed in aqueous KOH to produce the desired TTCA in 92% yield. Mp: 192.7–194.1 °C. IR (KBr) 1677, 2500–3100 (br) cm^{-1}; ^1H NMR (300 MHz, $CDCl_3$) δ: 7.04–7.59 (m, 7H), 7.59 (brs, 1H), ^{13}C NMR (75 MHz, $CDCl_3$) δ: 125.0, 125.9, 126.9, 127.8, 128.4, 128.6, 130.2, 133.6, 135.9, 136.1, 143.8, 166.7; MS mz^{-1} (rel intensity) 292 (M^+, 100%).

DATT was synthesized from 2,5-dibromo-3,4-dinitrothiophene by a two-step process. The Stille coupling reaction [19] of 2,5-dibromo-3,4-dinitrothiophene with tributyl(2-thienyl)stannane in the presence of catalytic $Pd(PPh_3)_2Cl_2$ produced the dinitro compound in 60% yield. The reduction of the nitro compound with $SnCl_2$ in EtOH–HCl produced a diamine compound (DATT) in 60% yield. Mp: 96–97 °C. IR (KBr) 3220 ($-NH_2$) cm^{-1}; ^1H NMR (300 MHz, $CDCl_3$) δ: 3.72 (m, 4H), 7.05–7.09 (m, 4H), 7.25 (dd, J = 1.5, 4.9 Hz, 2H), ^{13}C NMR (75 MHz, $CDCl_3$) δ: 110.0, 123.9, 124.0, 127.7, 133.6, 135.9; MS mz^{-1} (rel intensity) 273 (M^+, 100%).

2.2. Apparatus and materials

The cyclic voltammograms were recorded using a potentiostat/galvanostat, Kosentech Model PT-1 and EG & G PAR Model

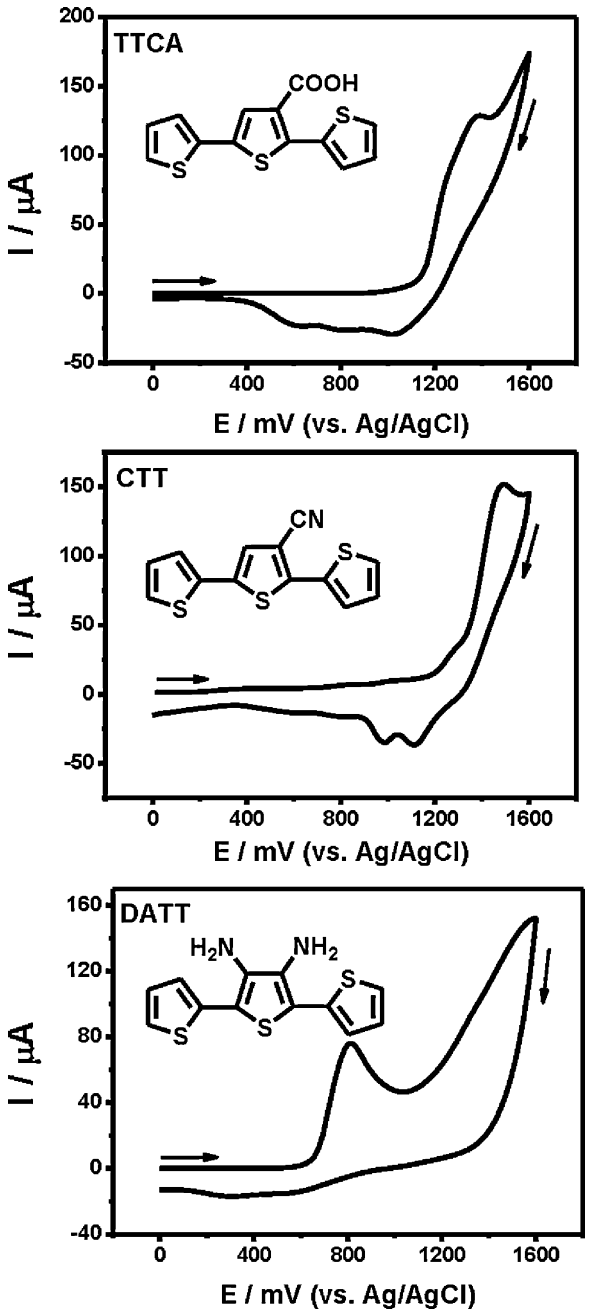

Fig. 1. Cyclic voltammograms for the electropolymerization of 1.0 mM terthiophene (TTCA, CTT, and DATT) in a 0.1 M TBAP dichloromethane solution from 0.0 to 1.6 V at scan rate of 100 mV s^{-1}. Inset: Structure of terthiophene monomers considered in this study.

PAR 273A. The impedance spectra were measured with the EG&G Princeton Applied Research PARSTAT 2263 at an open-circuit voltage from 100 kHz to 100 mHz and, at a sampling rate of five points per decade (AC amplitude: 10 mV). The UV–visible spectra were obtained using a UV-3101PC, Shimadzu. The SEM images were obtained with a Cambridge Stereoscan 240 at KBSI (Busan, South Korea). Atomic force microscope (AFM) images were obtained with a Digital Instrument Nanoscope™ 3D ADC5, Multimode (Veeco Instruments Inc., CA) operating in the tapping mode. A JEOL JEM-2010 electron microscope (Jeol High-Tech. Co.) with an acceleration voltage of 200 kV was used to obtain the TEM images. X-ray photoelectron spectroscopy (XPS) was performed using a VG Scientific ESCALAB 250 XPS spectrometer with a monochromated Al K_α

source with charge compensation at KBSI (Busan, South Korea). The photovoltaic measurements were performed using an air mass (AM) 1.5 solar simulator that was equipped with a 150 W xenon lamp (Model 92251A, Newport). The power of the simulated light was calibrated to 100 mW cm^{-2} using a reference Si photodiode, which was measured at the solar-energy institute (NREL (USA)). The short-circuit photocurrent of the reference Si solar cell was calibrated to the average data from NREL under the one-sun condition. The *I–V* curves were obtained by measuring the generated photocurrent using a Keithley Model 2400 digital source meter. The voltage step and delay time of the photocurrent were 10 mV and 40 ms, respectively.

Tetrabutylammonium perchlorate (TBAP, electrochemical grade) was received from Fluka (USA) and purified according to the general method; it was dried under vacuum at 1.33×10^{-3} Pa over 24 h. Dichloromethane (99.8%, anhydrous, sealed under N_2 gas) was received from Sigma Co. (USA). The fluorine-doped SnO_2 (FTO, 2.2 mm 15 Ω sq^{-1}), TiO_2 (Ti-Nanoxide HT), the electrolyte (Iodolyte PN-50), the Pt paste (platisol), and the hot-melt film (SX 1170-60) were purchased from Solaronix (Switzerland).

2.3. Fabrication of polymer dye solar cells

The working electrode was a fluorine-doped SnO_2 (FTO) glass plate with a size of 30 cm × 30 cm. The FTO glass plate was cut into 2 cm × 3 cm pieces. The FTO glass was cleaned in a detergent solution using an ultrasonic bath for 15 min and then rinsed with water and ethanol to prepare the working electrode, which was coated with the conjugated polymer for the TiO_2-based solar cell. A transparent nanocrystalline layer was formed on the FTO glass plate using a doctor blade-printing TiO_2 paste and then dried for 1 h at 25 °C. Then, the layer was heated under airflow at 450 °C for 30 min. Subsequently, the TiO_2 electrodes were immersed in a 50 mM $TiCl_4$ aqueous solution, dried at 70 °C for 30 min, and sintered at 450 °C for 30 min. The thickness of the TiO_2 film coated on the FTO glass was 3.5 μm. Conducting polymer layers were formed on the TiO_2 electrode by electropolymerization of the monomers in a 0.1 M TBAP/CH_2Cl_2 solution using the potential cycling method. The TiO_2/FTO electrode was used as the working electrode; Ag/AgCl (in saturated KCl) was used as the reference electrode, and a platinum plate was used as the counter electrode. The electropolymerization of the monomer on the TiO_2 electrode was conducted separately in a 0.1 M TBAP/CH_2Cl_2 solution containing monomer from a voltage of 0.0–1.6 V. Then, the electrodes were washed with CH_2Cl_2 to remove the excess monomer. The area of the active polymer layer was 0.24 cm^2. A hole was drilled on the FTO glass to prepare the counter electrode. The Pt-counter electrode was deposited on FTO glass by coating the surface with a drop of Pt solution. The surface was then treated at 450 °C for 15 min. The polymer-covered TiO_2 and Pt-counter electrodes were assembled into a sealed sandwich-type cell through heating at 100 °C using a hot-melt film with a thickness of 60 μm in the space between the electrodes. A drop of the redox electrolyte containing I^-/I_3^- in a propionitrile was placed in the hole on the back of the counter electrode. Finally, the hole was sealed using the hot-melt film and the cover glass (1 mm thickness).

3. Results and discussion

3.1. Electropolymerization and characterization of poly(terthiophene)

As shown in Fig. 1, polymer films are formed through electropolymerization of each monomer (TTCA, CTT, and DATT) in a 0.1 M TBAP/CH_2Cl_2 solution using a potential cycling method from 0.0 to 1.6 V vs. Ag/AgCl at a scan rate of 100 mV s^{-1}. During the polymerization, the oxidation peak of the TTCA monomer appears at 1.3 V at the first anodic scan, and the reverse scan to the negative potential shows a small cathodic peak at 0.9 V which corresponded to the reduction of the polymer film immediately formed on the electrode. For CTT, the oxidation peak is observed at 1.5 V, and the reverse scan shows two cathodic peaks at 1.1 and 0.97 V. For DATT, two oxidation peaks are observed at 0.75 and 1.35 V in the first anodic scan; the first peak corresponds to the oxidation of the amine group to an imine, and the second peak corresponds to the oxidation of the monomer to the polymer.

Fig. 2a shows a cross-section SEM image of the TiO_2 film in which the thickness of the TiO_2 layer is 3.5 μm. The surface morphology of the TiO_2 films after $TiCl_4$ treatment ($TiCl_4/TiO_2$) shows that the pore size of the TiO_2 film decreases, and the diameter of the particles increases (Fig. 2b). The particle size of the TiO_2 is determined to be 28.3 ± 5.8 nm. Improvements in the short-circuit photocurrent (J_{sc}) and the open-circuit voltage (V_{oc}) are observed after the $TiCl_4$ treatment [3,20,21]. The surface morphologies of poly-DATT (Fig. 2c), poly-CTT (Fig. 2d), and poly-TTCA (Fig. 2e) on the $TiCl_4/TiO_2$ films are obtained from the AFM images. The particle size of poly-DATT, poly-CTT, and poly-TTCA coated on the $TiCl_4/TiO_2$ films are determined to be 34.0 ± 10.2 nm, 28.5 ± 13.1 nm, and 56.5 ± 10.0 nm, respectively. These results indicate that the $TiCl_4/TiO_2$ electrode is covered with poly-TTCA more easily, and that the particle size of poly-TTCA/$TiCl_4/TiO_2$ (56.5 ± 10.0 nm) is larger than that of poly-DATT/$TiCl_4/TiO_2$ (34.0 ± 10.2 nm) and poly-CTT/$TiCl_4/TiO_2$ (28.5 ± 13.1 nm). Fig. 2f shows a cross-sectional image of the poly-TTCA layer formed around the TiO_2 particle using TEM where the thickness of the poly-TTCA layer was 12.5 nm.

Fig. 3 shows the XPS spectra in the region of C1s (Fig. 3a), Ti2p3 (Fig. 3b), and S2p (Fig. 3c) obtained for TiO_2/poly-CTT, TiO_2/poly-DATT, and TiO_2/poly-TTCA surfaces. The C1s spectra of poly-CTT and poly-DATT exhibit two peaks at 283.9 (C–C, C–H, and C–S bonds) and 285.2 eV (C–N bond or –CN group), whereas the C1s spectrum of poly-TTCA shows three peaks at 284.3 eV (C–C, C–H, and C–S bonds), 286.0 eV (C–O bond), and 288 eV (COOH group). The peaks of the poly-CTT and poly-DATT spectra appears at 283.9 eV due to C–C, C–H, and C–S bonds, and are shifted slightly to a higher energy of 284.3 eV for the poly-TTCA coated TiO_2 surface (TiO_2/poly-TTCA). In addition, a new peak appears at 286.0 eV for the TiO_2/poly-TTCA sample, which is due to C–O–Ti bond formation between poly-TTCA and TiO_2 [14–16]. The Ti2p3 spectrum exhibits a peak at 458.1 eV, due to the Ti–O bond. After polymer coating, the peak at 458.1 eV shifts slightly to a higher energy of 458.3 eV for TiO_2/poly-TTCA material due to the interaction between poly-TTCA and TiO_2. The S2p spectrum exhibits a peak at 163.5 eV due to the C–S bond of the polymer backbone. When coated with polymer dyes on the TiO_2 layer, the intensity of the S2p peak of poly-TTCA is stronger than that observed in poly-CTT and poly-DATT. This indicates that the amount of the poly-TTCA adsorbed onto the TiO_2 layer is much larger than that of poly-CTT or poly-DATT through the C–O–Ti bond formation of poly-TTCA and TiO_2.

3.2. Performance optimization of the polymer dye solar cells

The electropolymerization parameters for the formation of the polymer dye layers were optimized in terms of the number of potential cycles, the scan rate, and the monomer concentration to obtain a high energy conversion efficiency (ECE). Preliminary experiments showed that the best cell performance was achieved for poly-TTCA; therefore, the performance of the polymer dye cells was precisely optimized for poly-TTCA. Fig. 4a shows the ECE of the polymer (poly-TTCA/TiO_2) with respect to the potential cycles from 1 to 5 at a scan rate of 100 mV s^{-1} between 0.0 and 1.6 V in a 0.1 M TBAP/CH_2Cl_2 solution containing 1.0 mM monomer. The ECE rapidly decreases as the number of potential cycles increases.

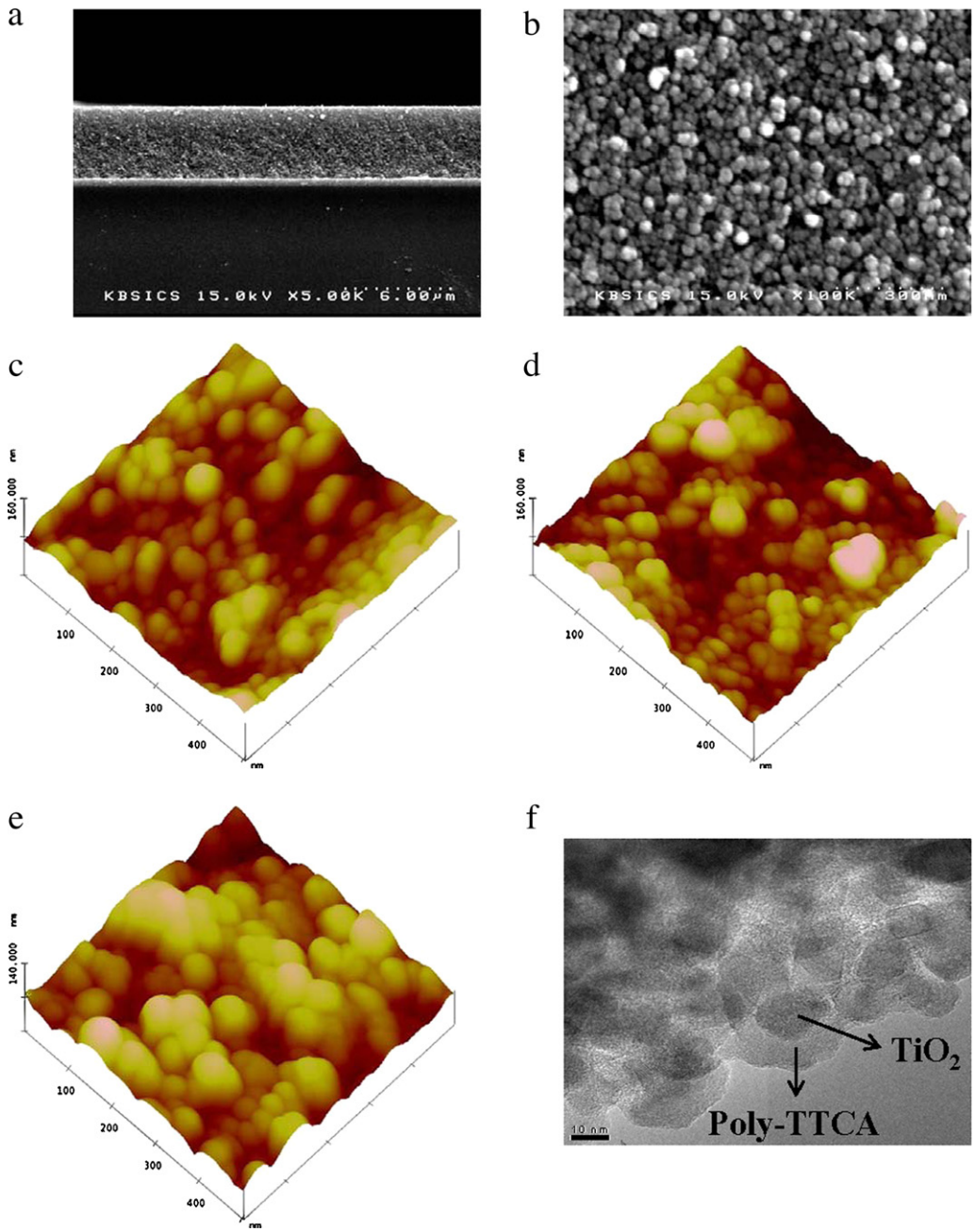

Fig. 2. SEM image showing a cross-section of (a) TiO_2 and a top view of (b) $TiCl_4/TiO_2$. AFM images of (c) poly-DATT/$TiCl_4/TiO_2$, (d) poly-CTT/$TiCl_4/TiO_2$, (e) poly-TTCA/$TiCl_4/TiO_2$. (f) TEM image of the formation of a poly-TTCA layer around a TiO_2 particle.

The maximum ECE (0.95%) is observed for one potential cycle. Thus, one cycle is chosen as the optimum number of potential cycles. Fig. 4b shows the ECE of the poly-TTCA/TiO_2 electrode as a function of scan rate from 50 to 200 mV s^{-1} in the monomer solution. The maximum ECE (0.95%) is observed at a scan rate of 100 mV s^{-1}; thus, this value is chosen as the optimum scan rate. The ECE as a function of the monomer concentration for polymerization was optimized over the concentration range of 1.0–20.0 mM in the monomer solution after a potential cycle from 0.0 to 1.6 V at a scan rate of 100 mV s^{-1}. The ECE gradually increases with increasing concentration from 1.0 to 5.0 mM. The ECE decreases, however, as the concentration increasing above 5.0 mM (Fig. 4c). The maximum ECE (2.32%) is observed at a monomer concentration of 5.0 mM. Therefore, the optimized electropolymerization concentration of the monomer is 5.0 mM in a 0.1 M TBAP/CH_2Cl_2 solution.

3.3. Bandgap energy of the polymer dyes

Fig. 5a shows the absorption spectra of the TTCA monomer, TTCA/TiO_2, and poly-TTCA/TiO_2 in a CH_2Cl_2 solution. The TTCA monomer exhibits a maximum absorption band, λ_{max}, at 342.9 nm, whereas the absorption bands of TTCA and poly-TTCA on the nanocrystlline TiO_2 film are observed at 368.5 nm and 447.6 nm, respectively [5]. A red-shift (25 nm for monomer and 100 nm for polymer) is observed for the absorption band of TTCA and poly-TTCA on the nanocrytalline TiO_2 film, implying that the polymerization and adsorption of the poly-TTCA occurred through the interaction with TiO_2. This interaction expedites the photoinduced charge transfer from poly-TTCA to TiO_2. The incident photon-to-current efficiency (IPCE) of the poly-TTCA solar cell is shown in Fig. 5b. The maximum IPCE value is 54.6% at 450 nm for the poly-TTCA component. The photocurrent is generated by photoin-

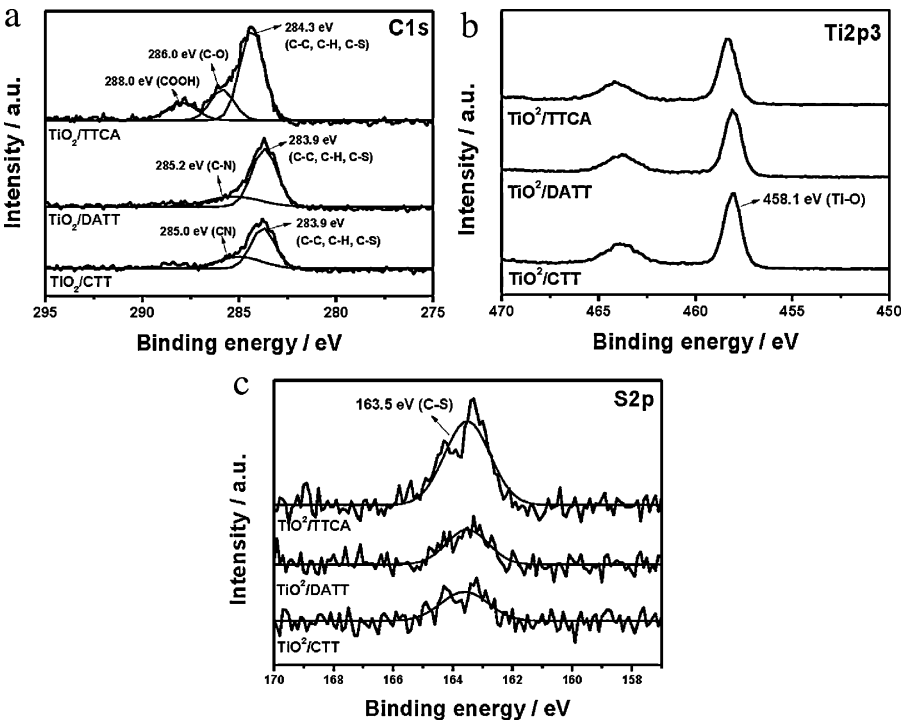

Fig. 3. ESCA spectra of (a) C1s, (b) Ti2p3, and (c) S2p peak for TiO_2/CTT, TiO_2/DATT, and TiO_2/TTCA.

duced electron transfer at the interface between the poly-TTCA and the nanocrystalline TiO_2.

The energy levels of poly-TTCA, poly-CTT, and poly-DATT are estimated from the cyclic voltmmograms and UV–visible absorption data. The oxidation potentials of TTCA, CTT, and DATT are used to determine the HOMO energy levels of the poly-TTCA, poly-CTT, and poly-DATT which are −5.59 eV, −5.75 eV, and −5.55 eV, respectively. From the absorption spectra, the bandgap energies of poly-TTCA, poly-CTT, and poly-DATT are 2.10 eV, 1.93 eV, and 2.09 eV, respectively. Therefore, the LUMO energy levels of −3.49 eV, −3.82 eV, and −3.46 eV (for poly-TTCA, poly-CTT, and poly-DATT, respectively) are estimated from the bandgap energies. The bandgaps of the polymers are similar in the range of 1.93–2.10 eV. Of these, the ECE of poly-TTCA on the nanocrystalline-TiO_2 solar cell is the highest at 2.32%. In the case of the poly-TTCA, the role of carboxylic groups on the monomer backbone has

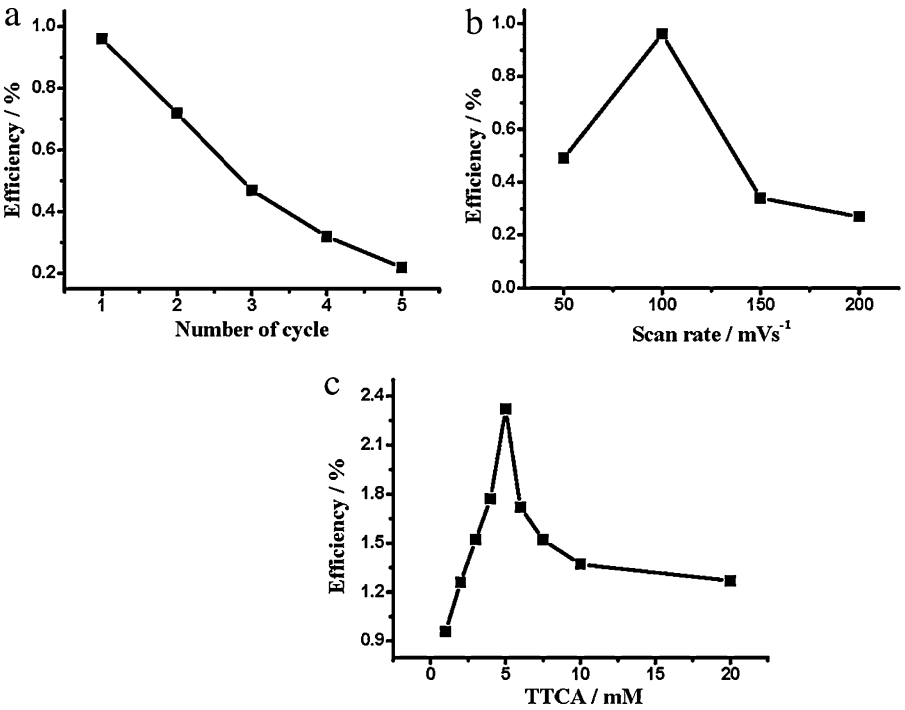

Fig. 4. The energy conversion efficiency of electropolymerization of TTCA on TiO_2 electrode at (a) the number of cycles, (b) various scan rates, and (c) various concentrations of TTCA monomer solution.

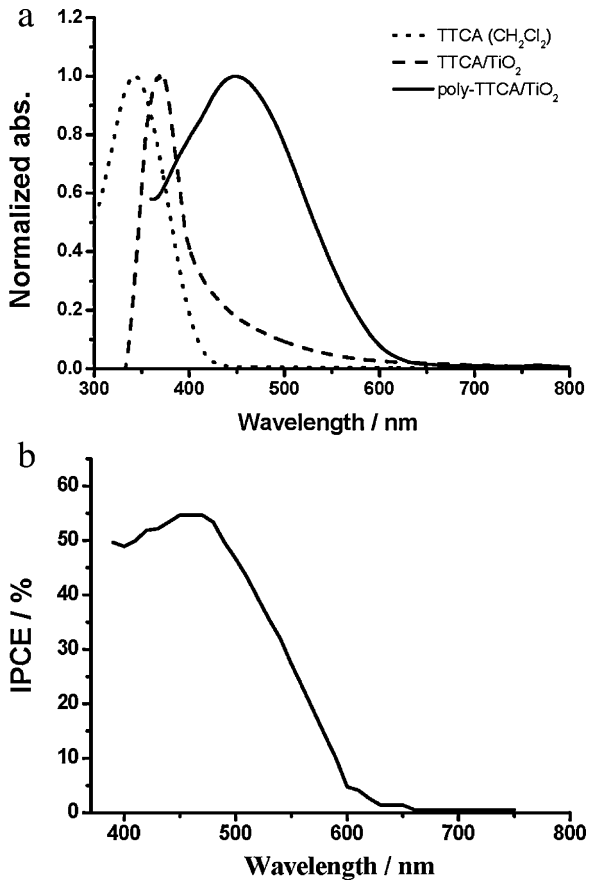

Fig. 5. (a) Absorption spectra of TTCA monomer solution (dot line), TTCA/TiO_2 (dashed line), and poly-TTCA/TiO_2 (solid line). (b) IPCE spectra of the poly-TTCA solar cell.

attracted attention as an efficient ligand for adsorption onto TiO_2, which would improve the transfer of the electrons from poly-TTCA to TiO_2.

3.4. Comparison of J–V characteristics of polymer dye solar cells

The photocurrent density–voltage (*J*–V) curves of the poly-TTCA-, poly-DATT-, and poly-CTT-sensitized solar cells are shown in Fig. 6. Table 1 shows the cell performance in terms of the short-circuit current (J_{sc}), the open-circuit voltage (V_{oc}), the fill factor (FF), and the energy conversion efficiency (η). The carboxylic acid group bearing the polymer, poly(terthiophene) (poly-TTCA), exhibits a higher energy conversion efficiency of 2.32% with a short-circuit current of 6.78 mA cm^{-2} and an open-circuit voltage of 0.54 V. The sensitizers without carboxylic acid groups, such as poly-DATT and poly-CTT, however, exhibit much smaller energy conversion efficiencies (0.14 and 0.16%, respectively) with low short-circuit currents of 0.51 and 0.62 mA cm^{-2}, respectively. For poly-TTCA, the carboxylic acid group is anchored strongly on the surface of the nanocrystalline TiO_2, which improves the electron transfer efficiency from poly-TTCA to TiO_2. The efficiency of 2.32% for poly-TTCA is greater than that previously reported using different kinds of polymers [5,6].

Table 1
Photoelectrochemical parameters obtained with a solar cell sensitized by conjugate polymers.

Device	J_{sc} (mA cm^{-2})	V_{oc} (V)	FF	η (%)
Poly-TTCA	6.78	0.54	63.6	2.32
Poly-DATT	0.51	0.41	65.6	0.14
Poly-CTT	0.62	0.41	64.5	0.16

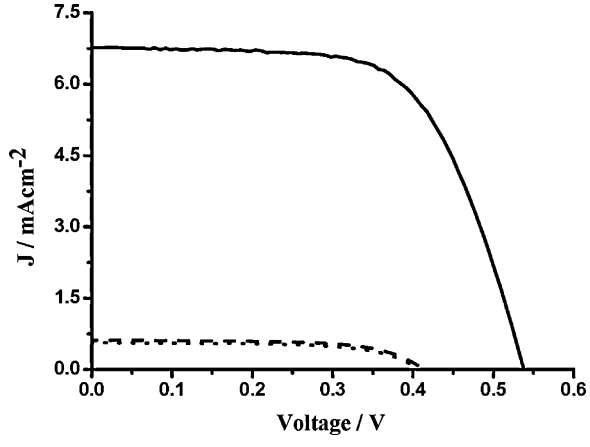

Fig. 6. The *J*–*V* characteristics of the poly-TTCA (solid line), poly-DATT (dotted line), and poly-CTT (dash line) as a sensitizer on a nanocrystalline TiO_2 solar cell under AM 1.5 condition.

3.5. Impedance spectroscopy of the polymer dye solar cells

Electrochemical impedance spectroscopy (EIS) is used to investigate the charge-transfer processes in various polymer dye solar cells at open-circuit voltage (−0.65 V vs. Ag/AgCl) in dark conditions. Fig. 7 shows the Nyquist plots obtained from poly-DATT, poly-CTT, and poly-TTCA dye solar cells. In the equivalent circuit, R_s represents the solution resistance, R_p1, R_p2, and R_p3 represent the polarization resistances, and *Q* is the constant-phase element (CPE; its parameters are Y_0, *n*). Values for the parameters of R_s, R_p1, R_p2, R_p3 and *Q* are obtained by fitting the experimental data to the equivalent circuit using Zview2 impedance software (Table 2). Two semicircles are observed for the polymer dye solar cells. This indicates that the polymer dye solar cells are composed of at least two different layers. Each semicircle can be assigned based on an equivalent circuit for the DSSCs. The smaller semicircle is observed corresponds to the charge-transfer processes occurring at the Pt/electrolyte (R_p1). The larger semicircles are composed of two layers, which correspond to the charge-transfer process at the TiO_2/polymers/electrolyte interface (R_p2) and in the electrolyte (R_p3) [22–24]. From the fitted values in Table 2, the poly-DATT and poly-CTT dye solar cells exhibits impedance values (R_p2) of 64.8 and 72.3 Ω, respectively, while the poly-TTCA shows the lowest impedance value of

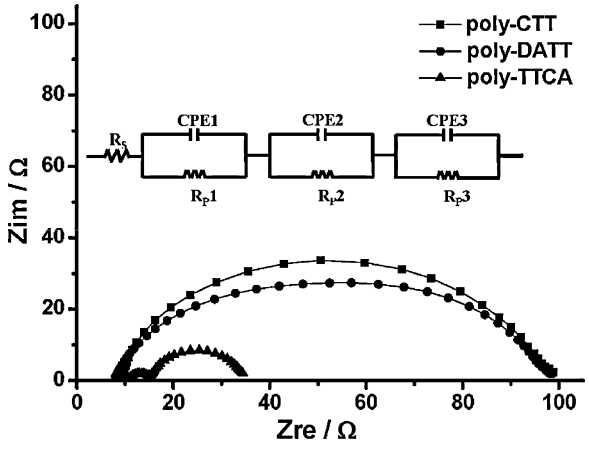

Fig. 7. Nyquist plots for poly-DATT, poly-CTT, and poly-TTCA dye solar cell at open-circuit voltage (−0.65 V). Inset: Equivalent circuit for polymer dye solar cells.

Table 2
The fitting values of the equivalent circuit element solar cell sensitized by polymer dye (poly-CTT, poly-DATT, and poly-TTCA).

	R_s, Ω	R_p1, Ω	Q_1		R_p2, Ω	Q_2		R_p3, Ω	Q_3	
			Y_0, mhg	n_1		Y_0, mhg	n_2		Y_0, mhg	n_3
Poly-TTCA	10.6	4.3	1.5×10^{-3}	1.1	15.5	1.7×10^{-3}	0.8	4.6	2.9×10^{-5}	0.9
Poly-DATT	7.7	7.0	1.6×10^{-5}	1.0	64.8	3.1×10^{-5}	0.8	7.9	1.5×10^{-5}	1.0
Poly-CTT	9.4	6.0	8.3×10^{-4}	0.9	72.3	1.2×10^{-5}	0.9	10.0	9.5×10^{-6}	1.0

15.5 Ω. This result indicates that poly-TTCA supports a relatively fast electron transfer in the TiO_2/polymer (poly-TTCA)/electrolyte interface, which should lead to greater energy conversion efficiency.

4. Conclusion

Poly(terthiophene) derivative-sensitized solar cells are successfully fabricated. The band gap energies of poly-TTCA, poly-CTT, and poly-DATT are similar in the range of 1.93–2.10 eV. Although the band gap energies are similar, however the carboxylic group containing poly(terthiophene) (poly-TTCA) exhibits a higher energy conversion efficiency than that of poly-CTT and poly-DATT. In the case of poly-TTCA, the anchoring group, −COOH can enhance the adsorption of the dye onto the TiO_2 layer effectively and strongly through the formation of C–O–Ti bonds, which improve the transfer of the electrons from poly-TTCA to TiO_2. Furthermore, poly-TTCA exhibits relatively fast electron transfer at the TiO_2/poly-TTCA/electrolyte interface, which should lead to greater energy conversion efficiency. The poly(terthiophene) derivative bearing carboxylic acid groups is the most efficient photosensitizer, and is a possible alternative materials to the Ru complexes. The maximum energy conversion efficiency of the poly-TTCA solar cell is 2.32% under an AM 1.5 solar simulated light irradiation of 100 mW cm^{-2}.

Acknowledgment

This work was supported by the Mid-career Researcher Program through NRF grant funded by the MEST. (No. 2009-007-9376).

References

[1] M. Granström, K. Petritsch, A.C. Arias, A. Lux, M.R. Andersson, R.H. Friend, Nature 395 (1998) 257–260.
[2] B. O'Regan, M. Grätzel, Nature 353 (1991) 737–740.
[3] M.K. Nazeeruddin, A. Kay, I. Rodicio, R. Humphry-Baker, E. Müller, P. Liska, N. Vlachopoulos, M. Grätzel, J. Am. Chem. Soc. 115 (1993) 6282–6390.
[4] A. Hagfeldt, G. Boschloo, L. Sun, L. Kloo, H. Pettersson, Chem. Rev. 110 (2010) 6595–6663.
[5] A.C. Arango, L.R. Johnsoe, V.N. Bliznyuk, Z. Schlesinger, S.A. Carter, H.H. Hörhold, Adv. Mater. 12 (2000) 1689–1692.
[6] Y.G. Kim, J. Walker, L.A. Samuelson, J. Kumar, Nano Lett. 3 (2003) 523–525.
[7] J. Liu, E.N. Kadnikova, Y. Liu, M.D. McGehee, J.M.J. Fréchet, J. Am. Chem. Soc. 126 (2004) 9486–9487.
[8] J.K. Mwaura, X. Zhao, H. Jiang, K.S. Schanze, J.R. Reynolds, Chem. Mater. 18 (2006) 6109–6111.
[9] G.K.R. Senadeera, T. Kitamura, Y. Wada, S. Yanagida, Sol. Energy Mater. Sol. Cells 88 (2005) 315–322.
[10] T. Yohannes, O. Inganäs, Synth. Met. 107 (1999) 97–105.
[11] C.A. Cutler, A.K. Burrell, G.E. Collis, P.C. Dastoor, D.L. Officer, C.O. Too, G.G. Wallace, Synth. Met. 123 (2001) 225–237.
[12] G. Tsekouras, C.O. Too, G.G. Wallace, Electrochim. Acta 50 (2005) 3224–3230.
[13] M. Vignali, R. Edward, V.J. Cunnane, J. Electroanal. Chem. 592 (2006) 37–45.
[14] R. Argazzi, C. Bignozzi, J. Inorg. Chem. 33 (1994) 5741–5749.
[15] Md.K. Nazeeruddin, S.M. Zakeeruddin, R. Humphry-Baker, M. Jirousek, P. Liska, N. Vlachopoulos, V. Shklover, C.-H. Fischer, M. Grätzel, J. Inorg. Chem. 38 (1999) 6298–6305.
[16] A. Hagfeldt, M. Grätzel, Acc. Chem. Res. 33 (2000) 269–277.
[17] T.Y. Lee, Y.B. Shim, S.C. Shin, Synth. Met. 126 (2002) 105–110.
[18] C. Kitamura, S. Tanaka, Y. Yamashita, Chem. Mater. 8 (1996) 570–578.
[19] J.K. Stille, Angew. Chem. Int. Ed Engl. 25 (1986) 508–524.
[20] N.G. Park, G. Schlichthörl, J. van de Lagemaat, H.M. Cheong, A. Mascarenhas, A.J. Frank, J. Phys. Chem. B 103 (1999) 3308–3314.
[21] P.M. Sommeling, B.C. O' Regan, R.R. Haswell, H.J.P. Smit, N.J. Bakker, J.J.T. Smits, J.M. Kroon, J.A.M. van Roosmalen, J. Phys. Chem. B 110 (2006) 19191–19197.
[22] C. Longo, A.F. Nogueira, M.-A. De paoli, J. Phys. Chem. B 106 (2002) 5925–5930.
[23] Q. Wang, J.-E. Moser, M. Grätzel, J. Phys. Chem. B 109 (2005) 14945–14953.
[24] J. Xia, N. Masaki, M. Lira-Cantu, Y.K. Kim, K. Jiang, S. Yanagida, J. Am. Chem. Soc. 130 (2008) 1258–1263.